

Estimating illumination coherence width from focused-probe intensity profiles

Armin Zjajo, Itai Matzkevich, Aram Rezikyan, Hongchu Du, Rafal Dunin-Borkowski

TESCAN
MIRA



FROM ROUTINE
TO REMARKABLE



Estimating illumination coherence width from focused-probe intensity profiles

Armin Zjajo¹, Itai Matzkevich², Aram Rezikyan³, Hongchu Du⁴ and Rafal Dunin-Borkowski⁵

¹Arizona State University, Phoenix, Arizona, United States, ²Arizona State University, United States,

³Corning, United States, ⁴Forschungszentrum Juelich GmbH, United States, ⁵Forchungszentrum Jülich, Nordrhein-Westfalen, Germany

Fluctuation Electron Microscopy (FEM) examines speckle in images and diffraction patterns that arises from constructive and destructive interferences between the waves scattered by atoms in the thin material. Strong coherence between the scattered waves is necessary if structural correlations between those atoms is to be detected [1]. High spatial coherence in the illumination is crucial.

Illumination spatial coherence can be controlled by adjusting the pre-specimen optics [2,3]. High spatial coherence generally results in low illumination fluence, and the scattered signals can be noisy. An additional concern is that atoms in the sample can move significantly during electron irradiation, and bulk motions also arise. Further, specimen charging, and the rapid motions of those charges, also contributes to this loss of coherence – or 'decoherence' – in the scattered beams, greatly degrading the speckle intensities. Experimentally, measured speckle variance is 10–100 times smaller than theory. To measure decoherence effects, calibration of the illumination spatial coherence is needed.

In our FEM studies using the scanning transmission FEM we have noticed that, although probes seem to have impressive numbers of Airy-intensity rings, the probe intensity profiles do not match well the idealized Airy intensity profile $2|J_1(qr)/qr|^2$, where q is 2π times the circular aperture radius (in reciprocal space) and r is radial position in the image plane. J_1 is the first-order Bessel function. Part of the issue seems to be saturation in the CCD camera near the high-intensity central 'Airy disk' portion of the probe. However, even the lower-intensity rings do not follow the idealized formula well.

Figure 1a shows a typical image of a focused probe, with no specimen present, using a logarithmic intensity scale to show the rings far from the center. It superficially resembles the Airy intensity function, shown in Figure 1b. However, intensity profiles reveal that the inner rings tend to appear as shoulders on the main central peak, and that the dips between rings do not fall anywhere near zero. Possible reasons for the discrepancies are: (1) The source is spatially incoherent; (2) strong lens aberrations, including defocus; (3) the non-linear response in the detector at high intensities.

To model the probes, we assume that the electron source can be treated as a surface of incoherent point emitters. This is not necessarily the surface of the emitter tip, but could be a virtual surface inside the tip from which emitted electrons can be back-projected to a point source. The distributed point sources are presumed to be mutually incoherent, and their density is distributed as a gaussian profile about some central point on the tip. The standard deviation of that gaussian, σ_c , is a measure of the angular spread of the tip as perceived at the focal plane. Each point source generates, in principle, its own Airy wave amplitude, with phase shifts across the wavefront introduced by tilt, as well as the aberrations in the lens system. These can be computed and the final intensity profile is, in effect, a convolution of the aberrated probe intensity profile with the gaussian emission profile across the tip.

The computed probe profile is compared to the experimental data by subtracting the two data sets and accumulating the square of the difference to generate a 'cost' function. Simulated annealing adjusts the various parameters (aperture radius, probe center, intensity scaling factor and offset, defocus, spherical aberration and astigmatism terms) to obtain the best fit between the model and experiment.

Our early results, based on probe intensity profiles, show that this approach is promising. The profiles in Fig. 1 and Fig. 2a show that the experimental fringe contrast fades quicker than for the ideal probe profile, although both intensities fade in proportion to $(qr)^{-3}$ (at large r), as expected for the Airy intensity profile (Fig. 2b). We find that our data is modeled fairly well as a convolution of the ideal Airy intensity with a narrow gaussian, the standard deviation of which, σ_A , is the reciprocal of the standard deviation of the gaussian emission profile, $\sigma_c = 1/\sigma_A$.

Our early attempts to model the probe profile entirely in terms of illumination spatial incoherence did not succeed in explaining all of the discrepancies. By concentrating our fitting function on the higher-order rings, along with a fitted zero-offset, we were able to obtain the fits shown in Figure 2a for two different probes. At large values of $x=qr$, the peaks in the ideal Airy intensity function should follow $|J_1(x)/x|^2 /x^3$. Figure 2b shows the same data multiplied by $x^3=(qr)^3$. Interpreting the discrepancy from the ideal probe as coming entirely from spatial incoherence, we infer that the spatial coherence angular widths relative to the aperture radii were 0.8 and 0.21 for probes 1 and 2, respectively. This is equivalent to about 1.5, and 23, incoherent sources illuminating the apertures, respectively. FEM uses low-resolution probes – typically 1.0 nm and bigger – which should be diffraction-limited. Nevertheless, a more accurate methodology may need to include wavefront aberrations, such as defocus, spherical aberration and astigmatism [3]. It has been pointed out that defocus can be an important issue [3], even for diffraction-limited probes. Temporal (longitudinal) incoherence may also be important in some experiments. We continue to refine our methods.

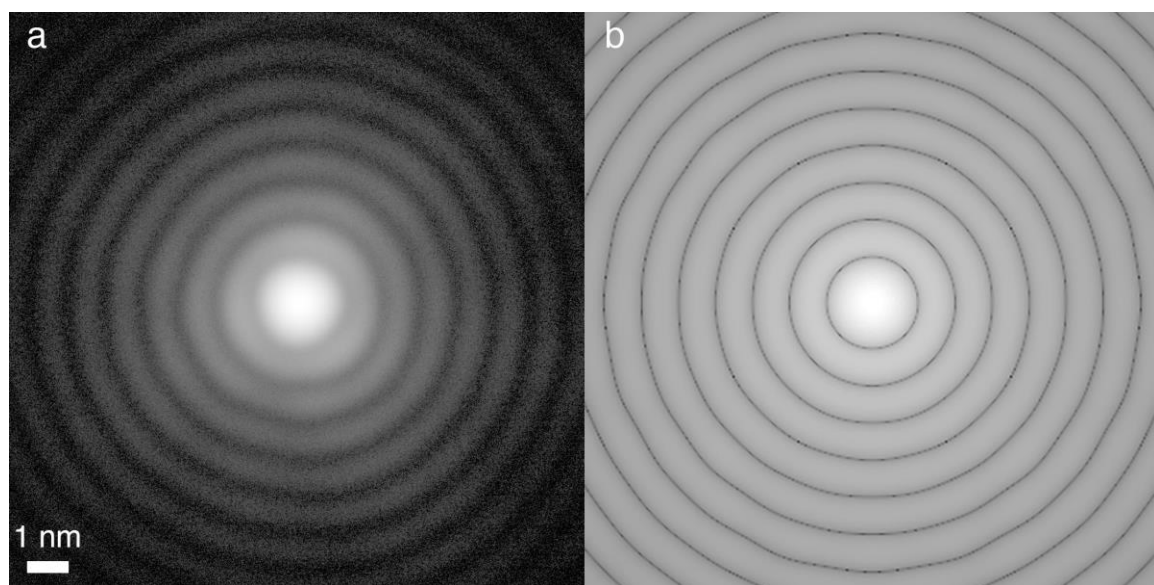


Figure 1. Probe intensity profiles (log scale) (a) Experimental. (b) Idealized Airy Intensity.

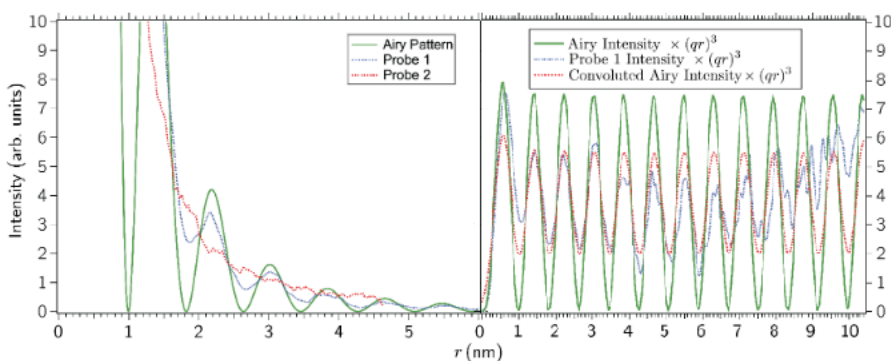


Figure 2. Two experimental probe intensity profiles (linear scale) compared with the Airy intensity profile. (a) Although Probe 1 (blue) has plentiful fringes (see FIG 1a), it does not match well the ideal Airy Pattern (green). (b) Probe intensity multiplied by $(qr)^3$. Experimental Probe 1 data (blue) can be modeled fairly well as a convolution of the ideal Airy intensity (green) with a narrow Gaussian to give the red plot. The reciprocal of the standard deviation of the gaussian is proportional to the spatial coherence width. Probe 2 fit is not shown.

References

1. M.M.J. Treacy et al., *Rep. Prog. Phys.*, 2005. **68**: p. 2899–2944.
2. P.M. Voyles and D.A. Muller, *Ultramicroscopy*, **93** 147–159 (2002).
3. D. Radic et al, *Microscopy and Microanalysis*, **26**, 1100-1109, (2020).